GEM TN-93-474
PITT/GEM 93-3

GEANT Monte Carlo Study of Long Strips in the GEM Endcap Calorimetry

Mark Clemen
University of Pittsburgh
Department of Physics and Astronomy

September 20, 1993

PITT/GEM 93-3
September 20, 1993

GEANT Monte Carlo Study of Long Strips in the GEM Endcap Calorimetry

Mark Clemen
University of Pittsburgh
Department of Physics and Astronomy

The purpose of this note is to present the pileup noise in long, 1.5 m by 5mm readout strips as a function of depth and of eta, for a few points in the EM section of the GEM endcap calorimeter. The peaking time used for this study is 50 *nsec*; the pileup sum S_p is $\approx$ 100 *nsec*. Such strips, placed at the shower maximum, are useful in determining the position (and angle with respect to the collision vertex) of the shower, and also have some π^0 rejection.

A simple calorimeter is modelled using GEANT with a strip readout. The calorimeter is a rectangular set of simple layers. The front consists of 1.2 X0 of aluminum, followed by alternating layers of 10mm of liquid argon and 4.23 X0 of lead. The box is placed in an SSC center-of-mass frame at various rapidities. The box is further tilted in some runs by 45 degrees to simulate the geometry of one cell of the accordion plates. The total energies deposited in 20 vertical strips 5mm by 1.5 meter are recorded in a data file.

The events are generated using ISAJET, at a low transverse momentum cutoff. The cross section of the simulation is estimated at 45 mb. The ISAJET runcards used are:

GEANT material	CUTELE	CUTGAM	DCUTE	BCUTE	cuts
Liquid Argon	10 keV	10 keV	10 keV	10 keV	low
Lead	10	10	10	100	
Liquid Argon	100	100	100	100	high
Lead	100	100	100	1000	

Table 1: GEANT Monte Carlo tracking and physics cutoffs used.

```
ISAJET RUNCARDS
40000., 1000, 3/
TWOJET
PT
5., 80./
NTRIES
1000./
END
STOP
```

By taking the total pp cross section at the SSC as 100 mb, the luminosity of the simulation is estimated to be 1.4 x $10^{33} cm^2/sec$. Since the pileup noise scales as the square root of the luminosity, the results of the simulation were multiplied by a factor of 2.67, to attain the pileup noise at a luminosity of $10^{34} cm^2/sec$.

Two sets of tracking cutoffs were used in the GEANT simulation for the liquid argon and the lead absorber. These are shown in Table 1. The higher cutoffs were thought to be accurate enough, and would give smaller fluctuations about the mean energy deposit RMS's. Actually the Gaussian sigmas about the RMS's found were as bad or worse for the higher cutoffs, in spite of the much better statistics. All cases were re-run using the lower cutoffs, although the results from the higher cutoffs are also presented here. There are some discrepancies between the results with the two sets of cutoffs; those with the lower cutoffs will be used.

Generous amounts of material on each side of the strips were included since fluctuations from shower spreading of nearby tracks contribute to the pileup noise as well. Some of the low energy tail of the shower spectrum is isotropic, and these particles can be reflected by adjacent material back into the strips, also necessitating modelling a larger volume.

The RMS of the energy deposited in the liquid argon is shown in the following Tables. All values shown represent deposited energies, i.e. there is no correction for the sampling fraction. These RMS's were found with full floating point statistics, and have no upper truncation as in a histogram. They are calculated for 4 strips centered on the rapidity as labelled. All are at least 10 cm from an edge boundary of the calorimeter. Initially, it was assumed that neighboring strips would have similar means and widths so their results could be averaged to improve statistial accuracy. However, using more strips in finding the average and its sigma, it was found that systematic changes were being introduced into the mean at the highest rapidity, and that the sigma was never improved for the larger statistics even at the lower rapidity. For these 4 strips, the mean energy deposit and its Gaussian sigma are presented separately.

Also presented here are the results of the 1st moment of these same energy deposits. The first column of each table shows this mean energy in each strip. Such means were previously interesting in the endcap calorimeter, as a gauge of the dc current that the preamps would typically draw. These are presented with any luminosity corrections.

Figures 1, 2 and 3 show the depth profiles of the pileup noise as a function of depth for each of the rapidities 1.74, 2.25, and 2.8, for a calorimeter facing the interaction region. An interesting feature in all three cases is the asymptotic value - the pileup noise of the shower even at great depths does not go to zero. Figures 4-6 show the same depth profiles, but for the calorimeter tilted by 45 degrees to mock one cell of the accordion calorimeter. Two things are apparent. The pileup noise is characteristically smaller in the accordion geometry. There is more material in some sense in this geometry for the shower to penetrate, but the shower RMS peak is at the same point as for the face-on case. The labelling in these 2 sets of figures is exactly the same; if one layer of absorber is 4.2 X0 thick, then n layers are n x 4.2 X0, and are labelled as such, regardless of whether there is an overall tilt. Note also that the asymptotic value in the tilted case now goes down very near to zero.

Since the pileup noise profiles vs. depth arise from fluctuations of the

energy deposits in EM showers, a similar parameterization as has been used previously was applied to them. This parameterization describes the number of secondary electrons with kinetic energy greater than 1.5 MeV in an electromagnetic shower crossing a plane at depth L, as have previously been fitted to GEANT results. We will ignore the actual values that were previously fitted, and re-fit to the pileup results.

$$N_{EM} L_X^{A_{EM}} e^{-B_{EM} L_X} \tag{1}$$

Here L_X is the depth in radiation lengths.

Unfortunately this was found to be insufficient to describe the calorimeter facing the origin, because of the slow falloff with depth in the simulation. The possibility that there are hadronic particles that are beginning to interact in the EM region of the calorimeter, adding to the tail of the pileup distribution is ruled out. The tilted configuration would show this also. Since the pileup results themselves are of order $\approx$ MeV, it is supposed that the energy cutoff in this parameterization is too high, that there is a lower energy component of the EM showers that is contributing appreciably to the pileup noise at larger depths. This same component is absorbed in the tilted configuration because of the greater amount of absorber material effectively facing particles travelling generally forward. Further, it is supposed that this lower energy component is spread more diffusely in depth, and that its peak is possibly, but not necessarily at the peak energy deposit.

The parameterization to fit the pileup noise with depth then is hypothesized to be of the form

$$N_{EM} L_X^{A_{EM}} e^{-B_{EM} L_X} + N_{LOW} e^{-(L_X - D_{LOW})^2/2W_{LOW}^2} \tag{2}$$

This equation was fit to all of the pileup results for each configuration (tilted or not) for all η's. In order to do so, a weighting with η had to be assumed. If one assumes that the pileup noise per unit (η, ϕ) is constant, then the change in each of (η, ϕ) vs. θ will weight the pileup noise. as one approaches the beam axis. The change in θ to η is just $\sin(\theta)$. The second factor, the change in ϕ, is similar. By measuring the pileup from a EM shower of fixed size in 3-space at some value θ, we are sampling some amount $\delta\phi$ as if some section of circumference about the beam axis at that θ we being sampled. If R_0 is the distance of this calorimeter cell from the origin, then the circumference of a circle there centered on the beam axis is

$$2\pi R_0 sin(\theta) \tag{3}$$

EM showers at smaller values of θ intersect larger values in ϕ, and would be expect to be larger by an amount $\sin(\theta_1)/\sin(\theta_2)$.

If θ then is taken as the smallest angle to the beam axis of the entire strip, then the weight of $1/\sin(\theta)^2$ from these two considerations was found to be to change too quickly to match the simulation results. See Table 16. Since the vertical strips sample many values of η, the integral of $1/\sin(\theta)$ must be calculated along this entire strip. This can be done exactly, and the full expected change in the pileup between strips was then fitted to a power law

$$weight = a_0\theta^{a_1} \tag{4}$$

where a_1 was found to be -1.376, with θ in radians. The full equation used for the pileup fitting then was

$$N_{EM}\theta^{a_1}L_X^{A_{EM}}e^{-B_{EM}L_X} + N_{LOW}\theta^{a_1}e^{-(L_X-D_{LOW})^2/2W_{LOW}^2} \tag{5}$$

Again see Table 16 for a full summary of the weightings discussed here.

Table 17 shows the results of fitting this equation using MINUIT to the set of depth profiles for the calorimetry in each configuration, with the lower tracking cutoffs. The χ^2 presented in the table is the total, not divided by the number of degrees of freedom. The fitting was first done for all η's for the no-tilt case. The first line is for the full fit, the second assumed that the proposed low-energy component peaked at the same depth as the peak seen in the Figures. The next two lines show the fitting results for the tilted (accordion-like) configuration. In both configurations, the total χ^2 is much better for the full fitting. There was some attempt to impose the same shape parameters in the fitting on the two sets of pileup noise, but the two configurations give results so different that the tails were reproduced very poorly in one or the other. The last two lines show the final fits used for the two configurations. These are the same fitting results as are shown in Figures 1-6. All fitting was done with the simulation results at the higher tracking cutoffs, as a cross check. The fitting was comparable.

Figures 1 and 2 shows good agreement with the fitting for the no-tilt case while Figure 3 shows a poorer agreement, at higher η. There may be a energy-dependent term in the fitting that should be added. The fits to the tilted-cell case show better agreement, although the error bars on the simulation results are large. The higher η case agrees better at the larger depths than the no-tilt case. Again, there may be some evidence for a longer falloff with depth in the pileup noise, than this ad-hoc second term in equation 5 accounts for.

1 Conclusions

The pileup noise in some proposed vertical 1.5m long strips has been investigated in the GEM endcap calorimeter using a full GEANT simulation with low cutoffs. The simulation results are match the expected rise as a function of η fairly well. The dependence on depth is roughly described by the same profile of peak as the total number of 1.5 MeV electron crossing some plane at depth L_X, although the tail on all distributions is longer. A phenomenological description of this as due to a lower-energy component of the shower led to a second term in the fitting, that seems to be born out in the data. There was no attempt to quantify the energy spectrum at each η, or to allow for shower shape peak changes in depth as that energy spectrum might shift towards higher values. Deeper penetration for higher energy particles may well be a larger component than assumed here.

We are indebted to Jim Russ, of Carnegie Mellon University, for donating the very generous amount of computer time and space necessary for such a large-scale Monte Carlo simulation. This work was supported in part by TNRLC grant No. RGFY92-109.

Material	Mean	@ 10^{34}	RMS	RMS @ 10^{34}	Pileup Noise
	KeV	KeV	KeV	MeV	MeV
1.2 X0 Al	33 ± 17	89 ± 46	561 ± 310	1.50 ± .83	3.74 ± 2.07
1.2 X0 + 4.23 X0	247 ± 36	661 ± 96	1466 ± 307	3.91 ± .82	9.78 ± 2.05
1.2 X0 + 8.46 X0	127 ± 16	339 ± 43	841 ± 96	2.25 ± .26	5.61 ± .66
1.2 X0 + 12.7 X0	66 ± 5	176 ± 14	602 ± 85	1.61 ± .23	4.02 ± .57
1.2 X0 + 16.9 X0	36 ± 6	97 ± 15	422 ± 68	1.13 ± .18	2.82 ± .45
1.2 X0 + 21.2 X0	39 ± 14	105 ± 38	507 ± 267	1.35 ± .71	3.38 ± 1.78
1.2 X0 + 25.4 X0	25 ± 8	66 ± 20	402 ± 265	1.07 ± 0.71	2.8 ± 1.77
1.2 X0 + 29.6 X0	17 ± 6	45 ± 15	296 ± 160	0.79 ± 0.43	1.98 ± 1.07

Table 2: GEANT RMS summary for 5mm strips, 10mm Liquid Argon depths, for a box calorimeter FACING the interaction region, at η=1.74. This simulation used the HIGHER energy tracking cutoffs.

Material	Mean	@ 10^{34}	RMS	RMS @ 10^{34}	Pileup Noise
	KeV	KeV	KeV	MeV	MeV
1.2 X0 Al	21 ± 5	55 ± 14	211 ± 86	0.57 ± .23	1.41 ± 1.57
1.2 X0 + 4.23 X0	215 ± 83	574 ± 222	1096 ± 521	2.93 ± 1.39	7.32 ± 3.48
1.2 X0 + 8.46 X0	117 ± 31	312 ± 83	540 ± 106	1.44 ± .28	3.60 ± .71
1.2 X0 + 12.7 X0	84 ± 26	223 ± 69	856 ± 410	2.29 ± 1.09	5.71 ± 2.74
1.2 X0 + 16.9 X0	30 ± 13	80 ± 35	208 ± 87	0.56 ± .23	1.39 ± .58
1.2 X0 + 21.2 X0	39 ± 46	104 ± 123	526 ± 728	1.41 ± 1.94	3.51 ± 4.86
1.2 X0 + 25.4 X0	20 ± 11	52 ± 29	214 ± 103	0.57 ± 0.27	1.42 ± 0.68
1.2 X0 + 29.6 X0	10 ± 3	26 ± 9	111 ± 26	0.30 ± 0.07	0.74 ± 0.18

Table 3: GEANT RMS summary for 5mm strips, 10mm Liquid Argon depths, for a box calorimeter FACING the interaction region, at η=1.74. This simulation used the LOWER energy tracking cutoffs.

Material	Mean	@ 10^{34}	RMS	RMS @ 10^{34}	Pileup Noise
	KeV	KeV	KeV	MeV	MeV
1.2 X0 Al	23 ± 13	61 ± 36	326 ± 276	.87 ± .74	2.18 ± 1.84
1.2 X0 + 4.23 X0	102 ± 13	273 ± 34	607 ± 101	1.62 ± .27	4.05 ± .67
1.2 X0 + 8.46 X0	70 ± 16	187 ± 44	736 ± 202	1.97 ± .54	4.91 ± 1.35
1.2 X0 + 12.7 X0	27 ± 4	73 ± 10	352 ± 159	.94 ± .42	2.35 ± 1.06
1.2 X0 + 16.9 X0	10 ± 5	26 ± 14	152 ± 83	.40 ± .22	1.01 ± .55
1.2 X0 + 21.2 X0	8 ± 6	21 ± 15	235 ± 285	.63 ± .76	1.57 ± 1.90
1.2 X0 + 25.4 X0	6 ± 7	15 ± 18	200 ± 262	0.53 ± 0.70	1.34 ± 1.75
1.2 X0 + 29.6 X0	2 ± 2	4.5 ± 3.9	55 ± 51	0.15 ± 0.14	0.36 ± 0.34

Table 4: GEANT RMS summary for 5mm strips, 10mm Liquid Argon depths, for a box calorimeter TILTED 45 degrees to the interaction region, at η=1.74. This simulation used the HIGHER energy tracking cutoffs.

Material	Mean	@ 10^{34}	RMS	RMS @ 10^{34}	Pileup Noise
	KeV	KeV	KeV	MeV	MeV
1.2 X0 Al	12 ± 6	33 ± 16	126 ± 56	.34 ± .15	0.84 ± 0.37
1.2 X0 + 4.23 X0	123 ± 11	328 ± 28	796 ± 232	2.13 ± .62	5.31 ± 1.55
1.2 X0 + 8.46 X0	52 ± 13	138 ± 34	402 ± 171	1.07 ± .46	2.8 ± 1.14
1.2 X0 + 12.7 X0	45 ± 10	121 ± 27	464 ± 238	1.24 ± .63	3.10 ± 1.59
1.2 X0 + 16.9 X0	20 ± 5	54 ± 14	301 ± 110	.80 ± .29	2.01 ± .73
1.2 X0 + 21.2 X0	3 ± 2	9 ± 7	64 ± 42	.17 ± .11	0.43 ± 0.28
1.2 X0 + 25.4 X0	1.4 ± 1.1	3.8 ± 2.9	31 ± 22	0.083± 0.059	.207 ± .147
1.2 X0 + 29.6 X0	6. ± 13.	18 ± 35	158 ± 313	.422 ± .836	1.06 ± 2.09

Table 5: GEANT RMS summary for 5mm strips, 10mm Liquid Argon depths, for a box calorimeter TILTED 45 degrees to the interaction region, at η=1.74. This simulation used the LOWER energy tracking cutoffs.

Material	Mean	@ 10^{34}	RMS	RMS @ 10^{34}	Pileup Noise
	KeV	KeV	KeV	MeV	MeV
1.2 X0 Al	101 ± 54	270 ± 144	729 ± 230	1.95 ± .61	4.87 ± 1.53
1.2 X0 + 4.23 X0	539 ± 45	1440 ± 119	2099 ± 192	5.60 ± .51	14.01 ± 1.28
1.2 X0 + 8.46 X0	339 ± 53	905 ± 140	1868 ± 585	4.99 ± 1.56	12.47 ± 3.91
1.2 X0 + 12.7 X0	186 ± 39	497 ± 105	1203 ± 537	3.21 ± 1.43	8.03 ± 3.58
1.2 X0 + 16.9 X0	151 ± 52	404 ± 138	1183 ± 854	3.16 ± 2.28	7.90 ± 5.70
1.2 X0 + 21.2 X0	103 ± 18	274 ± 49	881 ± 257	2.35 ± .68	5.88 ± 1.72
1.2 X0 + 25.4 X0	63 ± 4	167 ± 11	415 ± 81	1.11 ± 0.22	2.77 ± 0.54
1.2 X0 + 29.6 X0	66 ± 6	175 ± 15	696 ± 79	1.86 ± 0.21	4.64 ± 0.53

Table 6: GEANT RMS summary for 5mm strips, 10mm Liquid Argon depths, for a box calorimeter FACING the interaction region, at η=2.25. This simulation used the HIGHER energy tracking cutoffs.

Material	Mean	@ 10^{34}	RMS	RMS @ 10^{34}	Pileup Noise
	KeV	KeV	KeV	MeV	MeV
1.2 X0 Al	77 ± 34	206 ± 90	314 ± 102	.84 ± .27	2.09 ± .68
1.2 X0 + 4.23 X0	399 ± 85	1065 ± 228	1672 ± 420	4.47 ± 1.12	11.16 ± 2.80
1.2 X0 + 8.46 X0	254 ± 41	677 ± 110	1060 ± 395	2.83 ± 1.05	7.08 ± 2.64
1.2 X0 + 12.7 X0	135 ± 25	362 ± 66	593 ± 148	1.58 ± .40	3.96 ± .99
1.2 X0 + 16.9 X0	246 ± 125	656 ± 335	1807 ± 1260	4.82 ± 3.36	12.06 ± 8.41
1.2 X0 + 21.2 X0	80 ± 36	213 ± 96	433 ± 210	1.16 ± .56	2.89 ± 1.40
1.2 X0 + 25.4 X0	33 ± 12	87 ± 33	201 ± 38	0.54 ± 0.10	1.34 ± 0.25
1.2 X0 + 29.6 X0	41 ± 24	110 ± 63	253 ± 136	0.67 ± 0.36	1.69 ± 0.90

Table 7: GEANT RMS summary for 5mm strips, 10mm Liquid Argon depths, for a box calorimeter FACING the interaction region, at η=2.25. This simulation used the LOWER energy tracking cutoffs.

Material	Mean	@ 10^{34}	RMS	RMS @ 10^{34}	Pileup Noise
	KeV	KeV	KeV	MeV	MeV
1.2 X0 Al	38 ± 28	101 ± 75	622 ± 821	1.66 ± 2.19	4.15 ± 5.48
1.2 X0 + 4.23 X0	295 ± 30	788 ± 80	1581 ± 248	4.22 ± .66	10.56 ± 1.66
1.2 X0 + 8.46 X0	125 ± 8	334 ± 22	699 ± 129	1.87 ± .35	4.67 ± .86
1.2 X0 + 12.7 X0	120 ± 20	319 ± 54	1248 ± 590	3.33 ± 1.57	8.33 ± 3.94
1.2 X0 + 16.9 X0	57 ± 58	153 ± 156	998 ± 1340	2.67 ± 3.58	6.66 ± 8.94
1.2 X0 + 21.2 X0	16 ± 9	41 ± 23	293 ± 265	.78 ± .71	1.95 ± 1.77
1.2 X0 + 25.4 X0	9 ± 2	24 ± 3	142 ± 28	0.38 ± 0.07	0.95 ± 0.19
1.2 X0 + 29.6 X0	17 ± 13	45 ± 36	414 ± 417	1.10 ± 1.11	2.76 ± 2.78

Table 8: GEANT RMS summary for 5mm strips, 10mm Liquid Argon depths, for a box calorimeter TILTED 45 degrees to the interaction region, at η=2.25. This simulation used the HIGHER energy tracking cutoffs.

Material	Mean	@ 10^{34}	RMS	RMS @ 10^{34}	Pileup Noise
	KeV	KeV	KeV	MeV	MeV
1.2 X0 Al	30 ± 14	79 ± 37	245 ± 125	.65 ± .33	1.63 ± .83
1.2 X0 + 4.23 X0	307 ± 29	818 ± 79	1267 ± 313	3.38 ± .83	8.46 ± 2.09
1.2 X0 + 8.46 X0	202 ± 95	539 ± 253	1159 ± 568	3.09 ± 1.52	7.74 ± 3.79
1.2 X0 + 12.7 X0	59 ± 18	158 ± 47	354 ± 141	.95 ± .38	2.36 ± .94
1.2 X0 + 16.9 X0	14 ± 4	36 ± 10	108 ± 21	.29 ± .05	.72 ± .14
1.2 X0 + 21.2 X0	4 ± 5	10 ± 12	43 ± 50	.11 ± .13	.29 ± .33
1.2 X0 + 25.4 X0	1 ± 2	4 ± 6	19 ± 28	0.050 ± 0.074	0.12 ± 0.19
1.2 X0 + 29.6 X0	1 ± 1	1.6 ± 2.6	10 ± 15	0.026 ± 0.040	0.06 ± 0.10

Table 9: GEANT RMS summary for 5mm strips, 10mm Liquid Argon depths, for a box calorimeter TILTED 45 degrees to the interaction region, at η=2.25. This simulation used the LOWER energy tracking cutoffs.

Material	Mean	@ 10^{34}	RMS	RMS @ 10^{34}	Pileup Noise
	KeV	KeV	KeV	MeV	MeV
1.2 X0 Al	252 ± 68	673 ± 180	1154 ± 229	3.08 ± .61	7.70 ± 1.53
1.2 X0 + 4.23 X0	1525 ± 86	4072 ± 228	4714 ± 687	12.59 ± 1.83	31.47 ± 4.58
1.2 X0 + 8.46 X0	1030 ± 71	2749 ± 190	3338 ± 405	8.91 ± 1.08	22.28 ± 2.71
1.2 X0 + 12.7 X0	545 ± 62	1454 ± 165	2093 ± 157	5.59 ± .42	13.97 ± 1.05
1.2 X0 + 16.9 X0	298 ± 42	796 ± 112	1227 ± 309	3.28 ± .82	8.19 ± 2.06
1.2 X0 + 21.2 X0	224 ± 44	598 ± 117	1278 ± 390	3.41 ± 1.04	8.53 ± 2.60
1.2 X0 + 25.4 X0	201 ± 28	537 ± 75	1640 ± 565	4.38 ± 1.51	10.9 ± 3.8
1.2 X0 + 29.6 X0	176 ± 54	470 ± 144	1188 ± 370	3.17 ± .99	7.93 ± 2.47

Table 10: GEANT RMS summary for 5mm strips, 10mm Liquid Argon depths, for a box calorimeter FACING the interaction region, at η=2.8. This simulation used the HIGHER energy tracking cutoffs.

Material	Mean	@ 10^{34}	RMS	RMS @ 10^{34}	Pileup Noise
	KeV	KeV	KeV	MeV	MeV
1.2 X0 Al	364 ± 120	972 ± 320	1963 ± 1087	5.24 ± 2.90	13.1 ± 7.25
1.2 X0 + 4.23 X0	1626 ± 135	4340 ± 361	4876 ± 304	13.02 ± 0.81	32.6 ± 2.03
1.2 X0 + 8.46 X0	1060 ± 166	2831 ± 444	3108 ± 745	8.30 ± 1.99	20.75 ± 5.0
1.2 X0 + 12.7 X0	788 ± 179	2103 ± 478	3763 ± 1929	10.0 ± 5.2	25.2 ± 12.9
1.2 X0 + 16.9 X0	436 ± 50	1165 ± 132	2102 ± 372	5.61 ± 0.99	14.0 ± 2.48
1.2 X0 + 21.2 X0	356 ± 124	950 ± 330	2209 ± 1716	5.90 ± 4.58	14.7 ± 11.5
1.2 X0 + 25.4 X0	298 ± 96	796 ± 257	1629 ± 333	4.35 ± 0.89	10.9 ± 2.2
1.2 X0 + 29.6 X0	197 ± 66	527 ± 178	1091 ± 419	2.91 ± 1.12	7.28 ± 2.8

Table 11: GEANT RMS summary for 5mm strips, 10mm Liquid Argon depths, for a box calorimeter FACING the interaction region, at η=2.8. This simulation used the LOWER energy tracking cutoffs.

Material	Mean	@ 10^{34}	RMS	RMS @ 10^{34}	Pileup Noise
	KeV	KeV	KeV	MeV	MeV
1.2 X0 Al	133 ± 16	356 ± 43	1458 ± 417	3.89 ± 1.11	9.73 ± 2.78
1.2 X0 + 4.23 X0	697 ± 85	1862 ± 228	2538 ± 261	6.78 ± .70	16.94 ± 1.74
1.2 X0 + 8.46 X0	498 ± 64	1329 ± 170	2353 ± 505	6.28 ± 1.35	15.71 ± 3.37
1.2 X0 + 12.7 X0	244 ± 40	651 ± 107	1196 ± 249	3.19 ± .67	7.99 ± 1.66
1.2 X0 + 16.9 X0	79 ± 14	212 ± 38	592 ± 159	1.58 ± .42	3.95 ± 1.06
1.2 X0 + 21.2 X0	61 ± 29	162 ± 79	973 ± 746	2.60 ± 1.99	6.50 ± 4.98
1.2 X0 + 25.4 X0	32 ± 16	85 ± 42	424 ± 242	1.13 ± 0.65	2.83 ± 1.62
1.2 X0 + 29.6 X0	13 ± 7	34 ± 19	178 ± 110	0.47 ± 0.29	1.19 ± 0.73

Table 12: GEANT RMS summary for 5mm strips, 10mm Liquid Argon depths, for a box calorimeter TILTED 45 degrees to the interaction region, at η=2.8. This simulation used the HIGHER energy tracking cutoffs.

Material	Mean	@ 10^{34}	RMS	RMS @ 10^{34}	Pileup Noise
	KeV	KeV	KeV	MeV	MeV
1.2 X0 Al	52 ± 15	140 ± 40	252 ± 76	0.67 ± 0.20	1.68 ± 0.50
1.2 X0 + 4.23 X0	764 ± 248	2040 ± 662	2587 ± 708	6.91 ± 1.89	17.3 ± 4.73
1.2 X0 + 8.46 X0	497 ± 64	1326 ± 171	1732 ± 302	4.62 ± 0.81	11.6 ± 2.0
1.2 X0 + 12.7 X0	260 ± 84	694 ± 225	1403 ± 629	3.75 ± 1.68	9.37 ± 4.20
1.2 X0 + 16.9 X0	246 ± 214	657 ± 571	2884 ± 2910	7.70 ± 7.77	19.3 ± 19.4
1.2 X0 + 21.2 X0	34 ± 13	91 ± 34	209 ± 46	0.56 ± 0.12	1.40 ± 0.31
1.2 X0 + 25.4 X0	32 ± 8	85 ± 22	270 ± 76	0.72 ± 0.20	1.80 ± 0.51
1.2 X0 + 29.6 X0	11 ± 6	29 ± 16	126 ± 78	0.34 ± 0.21	0.84 ± 0.52

Table 13: GEANT RMS summary for 5mm strips, 10mm Liquid Argon depths, for a box calorimeter TILTED 45 degrees to the interaction region, at η=2.8. This simulation used the LOWER energy tracking cutoffs.

Material	Mean	@ 10^{34}	RMS	RMS @ 10^{34}	Pileup Noise
	KeV	KeV	KeV	MeV	MeV
1.2 X0 Al	5 ± 2	14 ± 6	84 ± 51	$.223 \pm .14$	$.558 \pm .34$
1.2 X0 + 4.23 X0	42 ± 10	113 ± 26	355 ± 101	$.95 \pm .27$	$2.37 \pm .67$
1.2 X0 + 8.46 X0	10 ± 1	28 ± 2	107 ± 12	$.285 \pm .031$	$.713 \pm .078$
1.2 X0 + 12.7 X0	4 ± 1	11 ± 4	61 ± 25	$.164 \pm .067$	$.410 \pm .168$
1.2 X0 + 16.9 X0	3 ± 5	8 ± 13	50 ± 66	$.134 \pm .177$	$.336 \pm .443$
1.2 X0 + 21.2 X0	6 ± 9	15 ± 24	143 ± 235	$.38 \pm .63$	$.96 \pm 1.57$

Table 14: GEANT summary for 1mm strips and 10mm Liquid Argon depth, for a box calorimeter TILTED 45 degrees to the interaction region, at η=2.25. This simulation used the HIGHER energy tracking cutoffs.

Material	Mean	@ 10^{34}	RMS	RMS @ 10^{34}	Pileup Noise
	KeV	KeV	KeV	MeV	MeV
1.2 X0 Al	374 ± 365	999 ± 974	1831 ± 855	4.89 ± 2.28	12.23 ± 5.71
1.2 X0 + 4.23 X0	1268 ± 409	3387 ± 1091	4939 ± 1558	13.19 ± 4.16	33.0 ± 10.4
1.2 X0 + 8.46 X0	831 ± 240	2218 ± 641	3630 ± 1468	9.69 ± 3.92	24.2 ± 9.8
1.2 X0 + 12.7 X0	588 ± 265	1570 ± 708	2888 ± 1424	7.71 ± 3.80	19.3 ± 9.5
1.2 X0 + 16.9 X0	396 ± 70	1057 ± 187	1757 ± 256	4.69 ± .68	11.7 ± 1.7
1.2 X0 + 21.2 X0	504 ± 138	1346 ± 368	3140 ± 1404	8.38 ± 3.75	21.0 ± 9.4
1.2 X0 + 25.4 X0	363 ± 109	970 ± 291	2192 ± 747	5.85 ± 1.99	14.6 ± 5.0
1.2 X0 + 29.6 X0	321 ± 122	857 ± 325	1868 ± 802	4.99 ± 2.14	12.5 ± 5.4

Table 15: GEANT RMS summary for 25mm strips, 10mm Liquid Argon depths, for a box calorimeter tilted 45 degrees to the interaction region, at η=2.25. This simulation used the HIGHER energy tracking cutoffs.

η	θ	$1/\sin(\theta)$	$1/\sin(\theta)^2$	integral^2	fit
1.74	.3491	1.0	1.0	1.0	1.0
2.25	.2094	1.65	2.70	2.16	2.02
2.8	.1215	2.82	7.96	4.28	4.27

Table 16: The expected weighting describing the pileup dependence with η is calculated exactly in the column titled 'integral^2', with a power law fitting shown in the next column.

tilt	χ^2	N_{EM}	A_{EM}	B_{EM}	N_{LOW}	D_{LOW}	W_{LOW}
0.	35.8	.0147 ± .003	6.26 ± .25	1.12 ± .037	.488 ± .046	13.6 ± .88	11.2 ± .62
0.	41.1	.0044 ± .0003	7.17 ± .04	1.18 ± .012	.382 ± .063	EM depth	20.0 ± 3.1
45	20.5	.115 ± .027	2.77 ± .30	.465 ± .053	.062 ± .018	24.8 ± 1.2	3.9 ± 1.3
45	36.3	.120 ± .026	2.42 ± .22	.390 ± .033	.0 ± .0082	EM depth	10. ± 52.
45	29.2	.012 ± .0012	6.26 fixed	1.12 fixed	.136 ± .024	9.6 ± 2.0	11.4 ± 2.1
0.	43.6	.167 ± .016	2.77 fixed	.465 fixed	.239 ± .060	19.4 ± 4.61	14.9 ± 6.13
0.	35.8	.0147 ± .003	6.26 ± .25	1.12 ± .037	.488 ± .046	13.6 ± .88	11.2 ± .62
45	20.5	.115 ± .027	2.77 ± .30	.465 ± .053	.062 ± .018	24.8 ± 1.2	3.9 ± 1.3

Table 17: MINUIT fit to pileup noise depth profiles using Eq. 5. These simulations used the LOWER tracking cutoffs, for both calorimeter configurations. The last two lines are taken here as the final fits to the simulations.

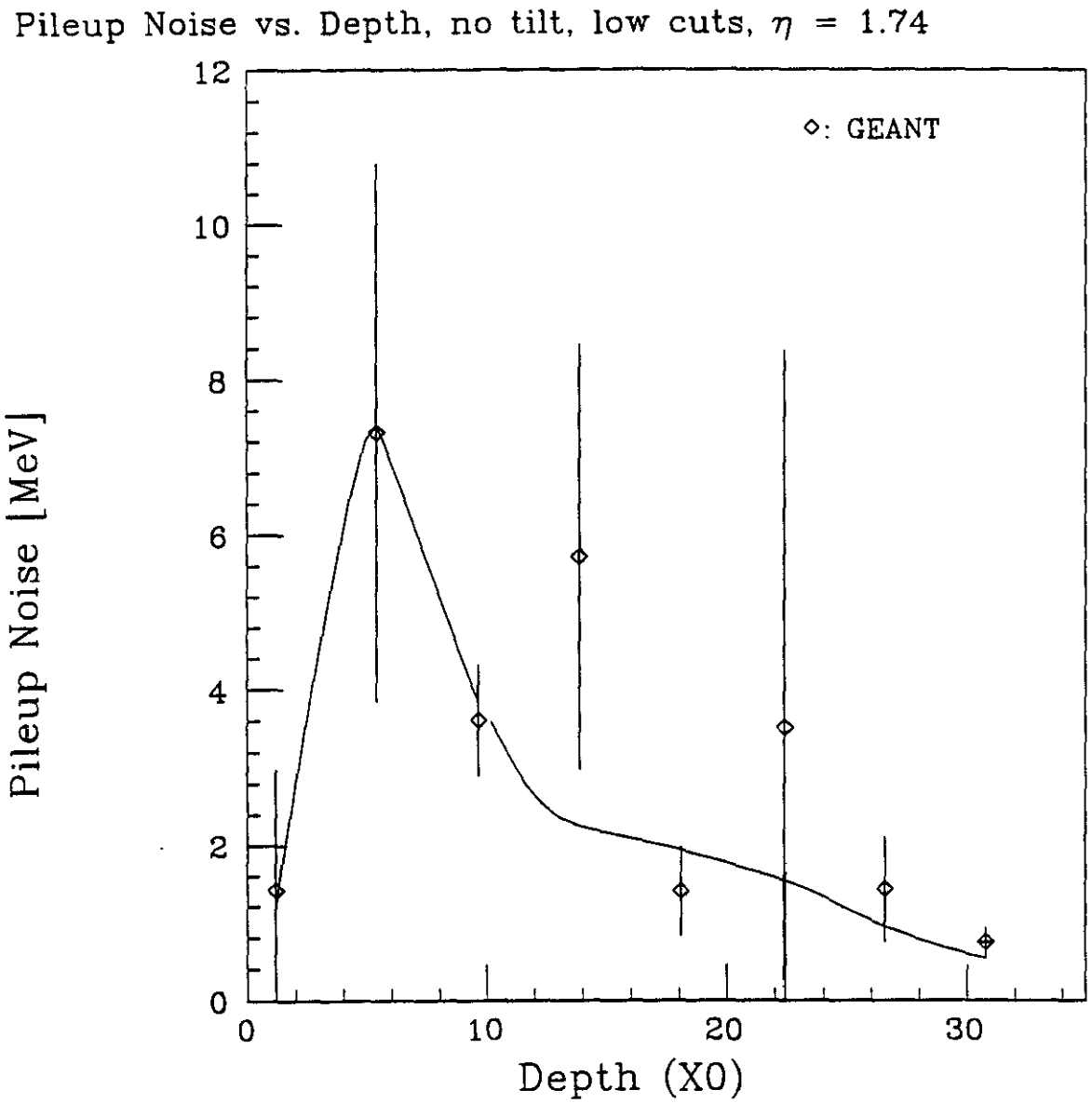

Figure 1: The Pileup Noise vs. Total Depth in a Lead/Liquid Argon Calorimeter Facing the origin at η=1.74, for ISAJET generated background at a luminosity of 10^{34}. Also shown is a MINUIT fitting according to Eq. 5.

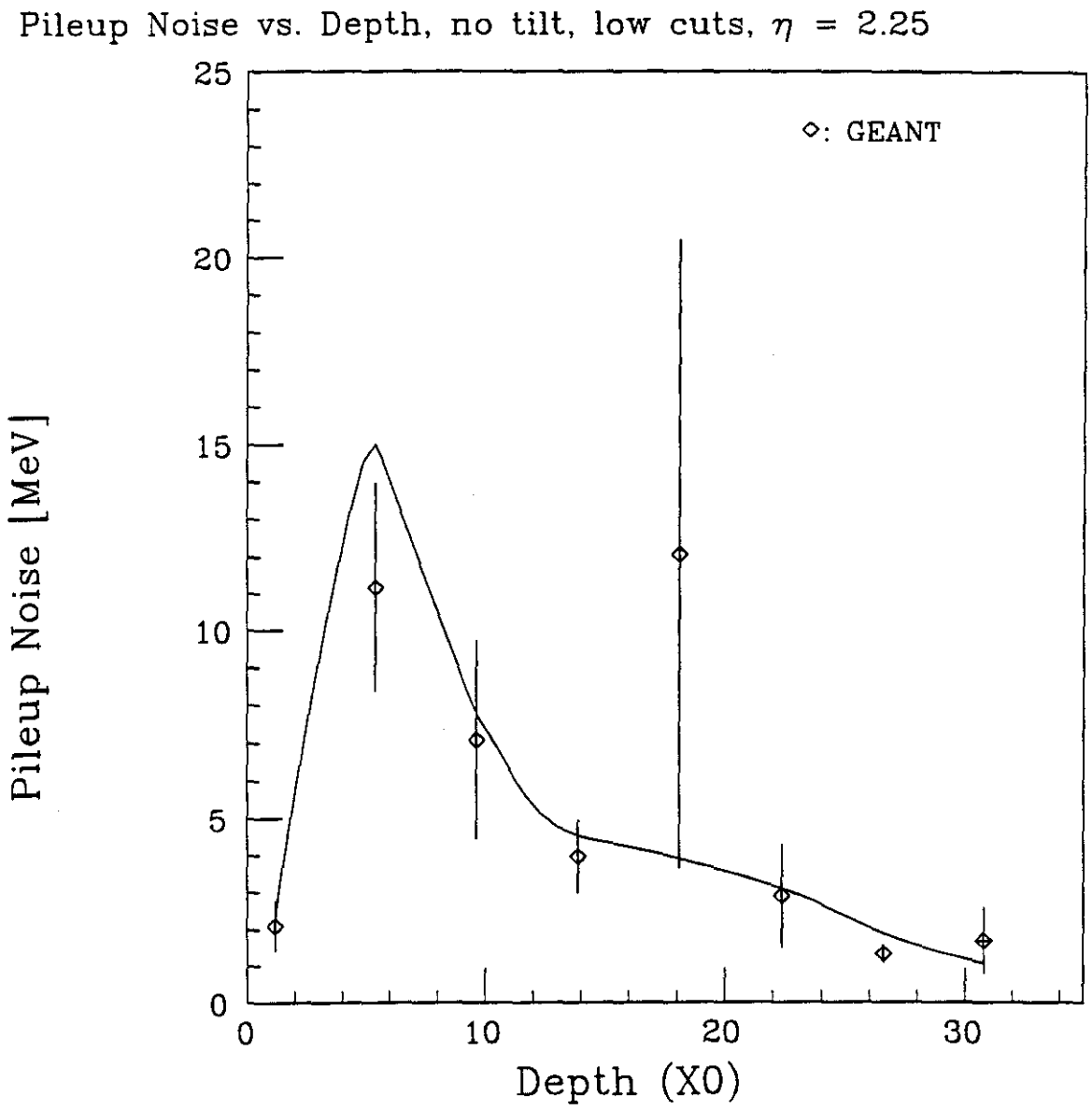

Figure 2: The Pileup Noise vs. Total Depth in a Lead/Liquid Argon Calorimeter Facing the origin at η=2.25, for ISAJET generated background at a luminosity of 10^{34}. Also shown is a MINUIT fitting according to Eq. 5.

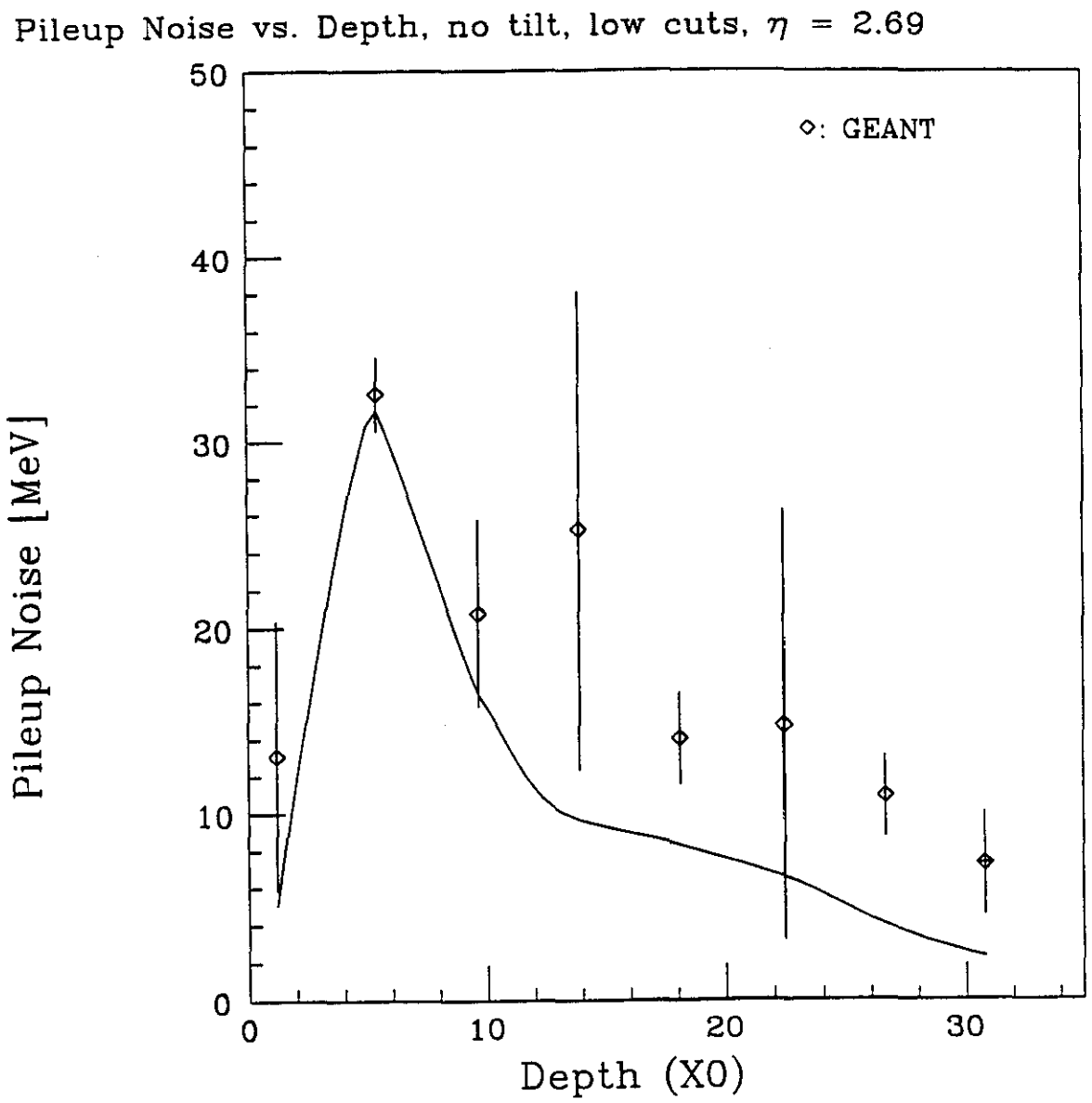

Figure 3: The Pileup Noise vs. Total Depth in a Lead/Liquid Argon Calorimeter Facing the origin at η=2.8, for ISAJET generated background at a luminosity of 10^{34}. Also shown is a MINUIT fitting according to Eq. 5. The fitting here is being pulled down by the previous results for η's of 1.74 and 2.25, since these were all fitted simultaneously.

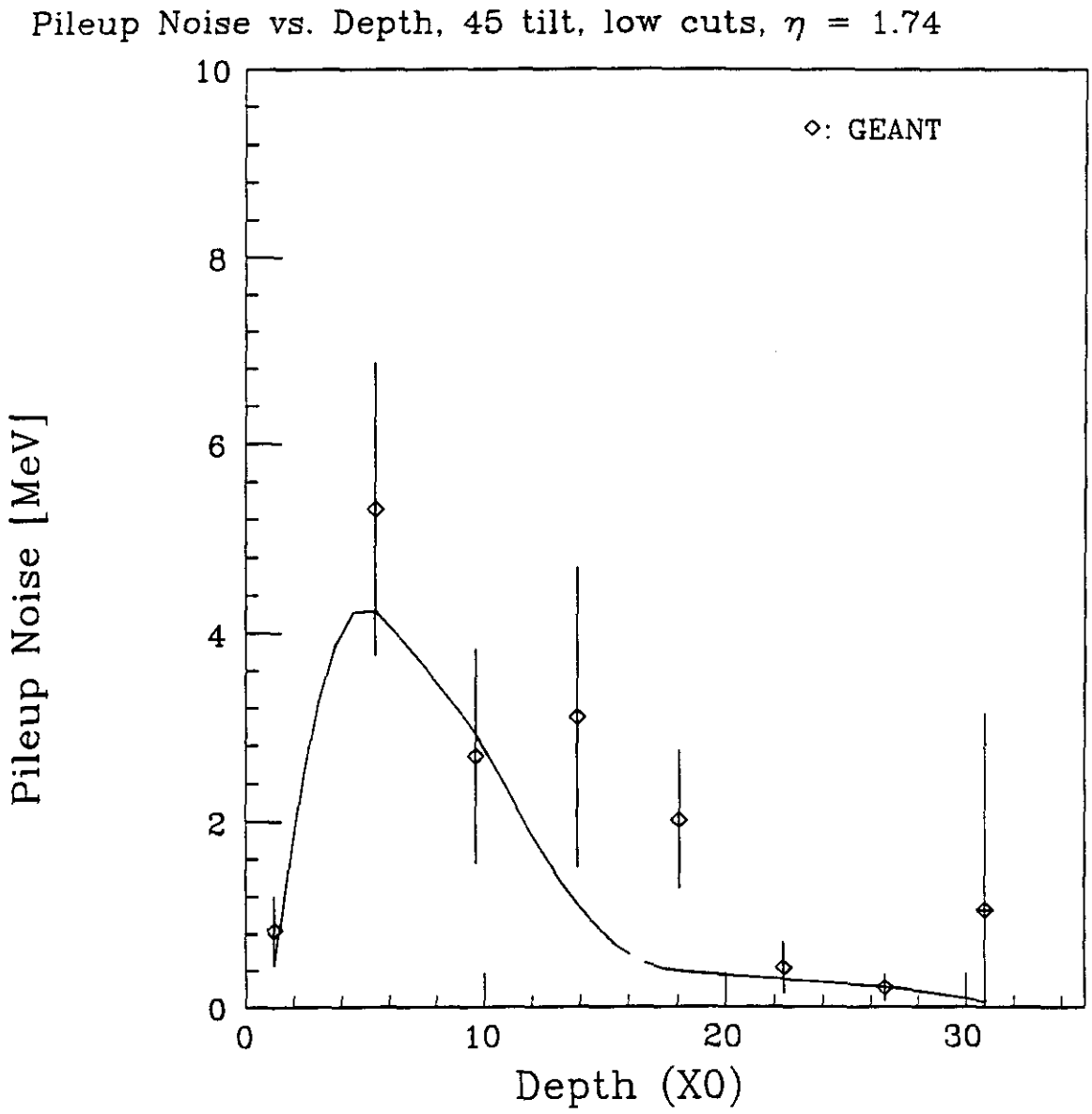

Figure 4: The Pileup Noise vs. Total Depth in a Lead/Liquid Argon Calorimeter Tilted 45 degrees with respect to the typical particles enterring the face, at η=1.74. The noise was found from ISAJET generated background corrected to a luminosity of 10^{34}. Also shown is a MINUIT fitting according to Eq. 5.

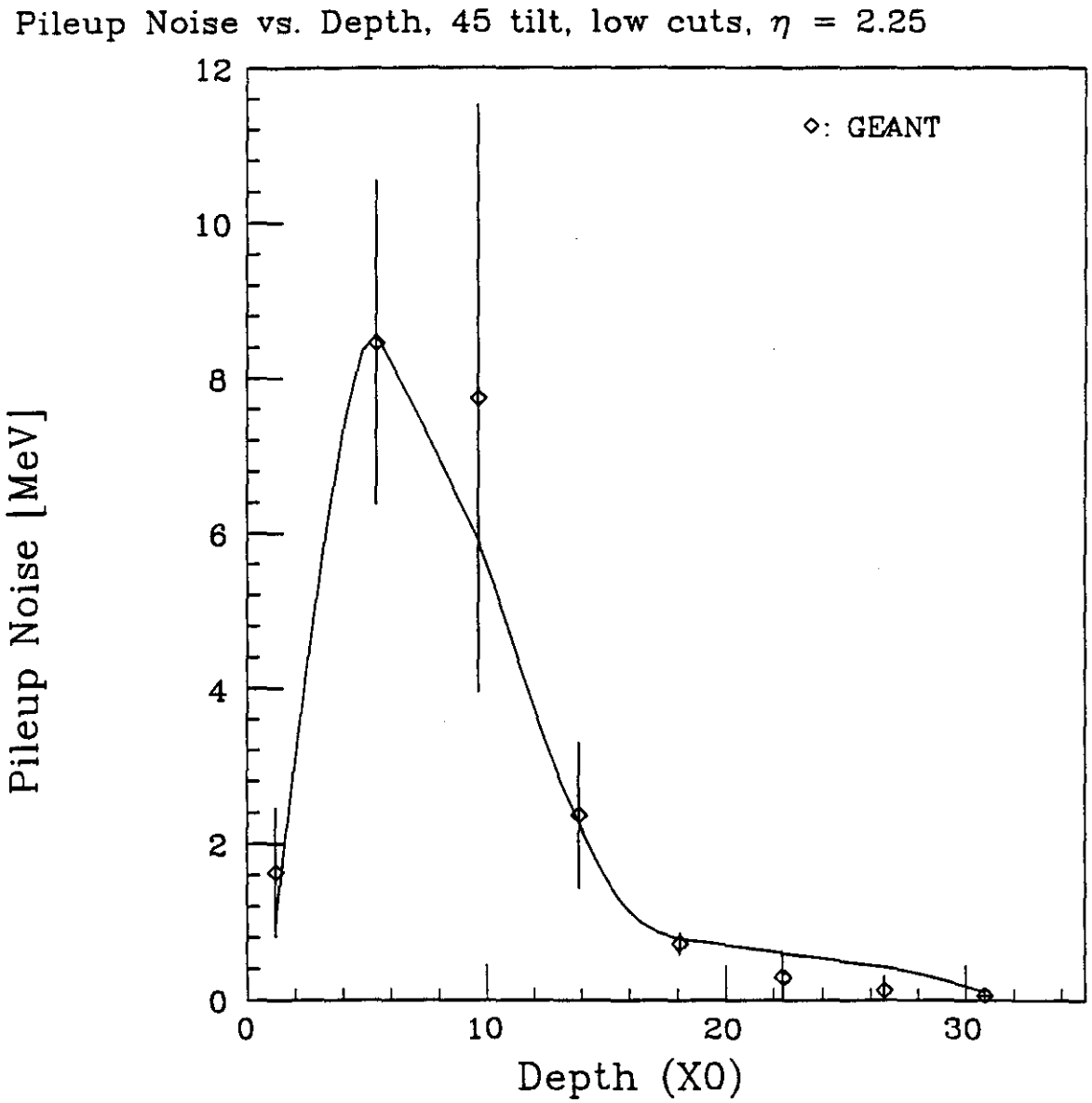

Figure 5: The Pileup Noise vs. Total Depth in a Lead/Liquid Argon Calorimeter Tilted 45 degrees with respect to the typical particles enterring the face, at η=2.25. The noise was found from ISAJET generated background corrected to a luminosity of 10^{34}. Also shown is a MINUIT fitting according to Eq. 5.

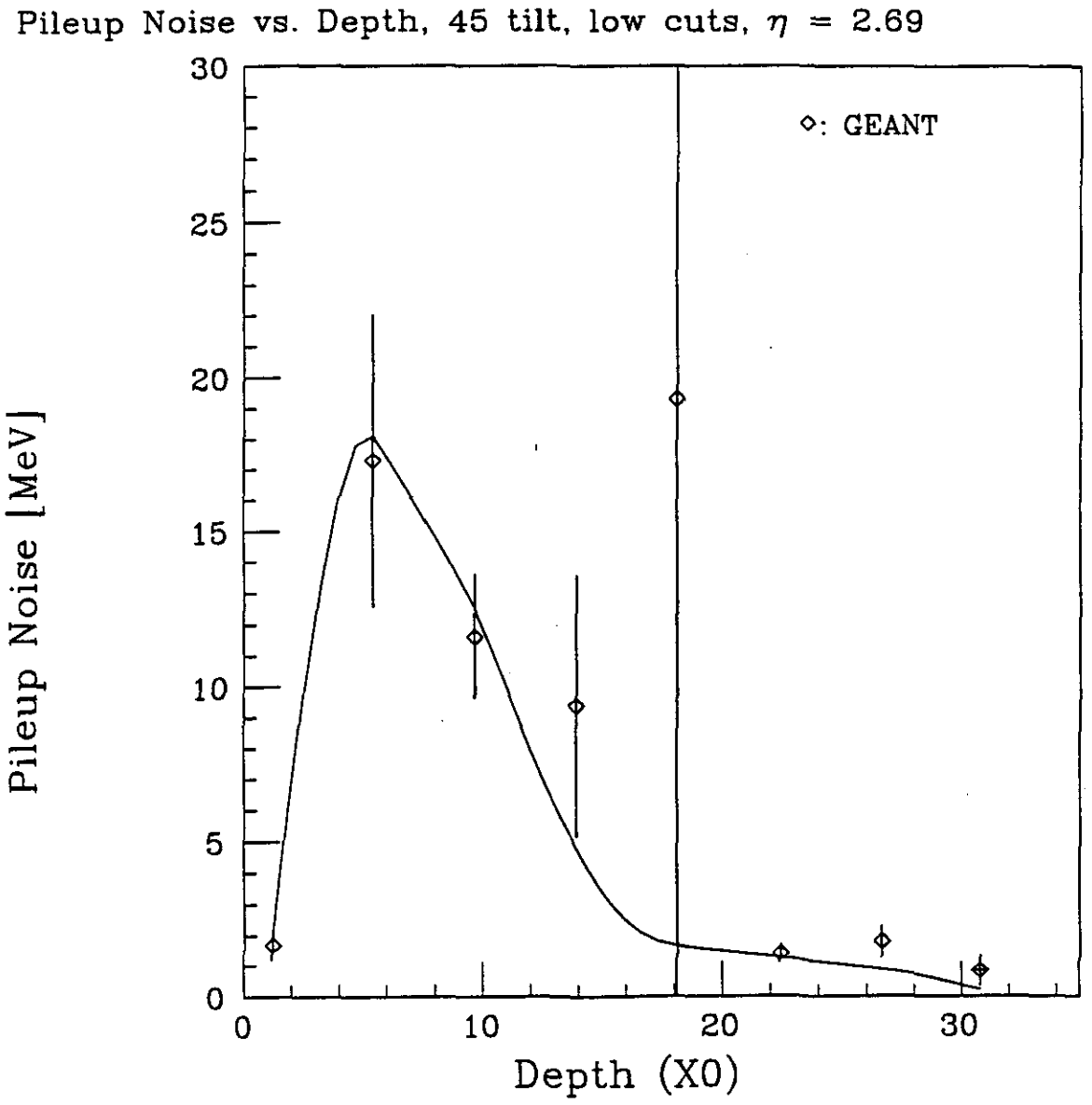

Figure 6: The Pileup Noise vs. Total Depth in a Lead/Liquid Argon Calorimeter Tilted 45 degrees with respect to the typical particles enterring the face, at η=2.69. The noise was found from ISAJET generated background corrected to a luminosity of 10^{34}. Also shown is a MINUIT fitting according to Eq. 5.